EVALUATION OF METHODS USED TO CALCULATE SEISMIC FRAGILITY CURVES

Prepared for

U.S. Nuclear Regulatory Commission
Contract No. NRC–HQ–12–C–02–0089

Prepared by

Biswajit Dasgupta

Center for Nuclear Waste Regulatory Analyses
San Antonio, Texas

May 2017

ABSTRACT

The U.S. Department of Energy (DOE) identified seismic hazards as credible natural hazards at the Yucca Mountain site during both the preclosure and postclosure periods. The preclosure period corresponds to approximately 100 years of operation before permanent closure of the repository, when the incoming waste would be handled at the surface facility structures for receiving, repackaging, aging, transporting, and placing in repository drifts. The preclosure safety analysis identified and quantified seismically initiating events and resulting event sequences associated with seismic hazards. This report documents the information collected and analyzed as part of the preparatory activities assisting the review of the DOE preclosure safety analysis.

The U.S. Nuclear Regulatory Commission issued Interim Staff Guidance (ISG) HLWRS-ISG-01 for review of seismically initiated event sequences in the preclosure safety analysis. The review methodology in the ISG considers both the likelihood of seismic initiating events at the site, and the fragility of structures, systems, and components (SSCs) important to safety (ITS). The analysis is intended to estimate the probability of failure of SSCs ITS and frequency of occurrence of event sequences. In the ISG, seismic fragility of a structure or equipment is defined as the conditional probability of failure for a given level of seismic ground motion, either defined as the peak ground acceleration (PGA) or a spectral ground acceleration (Sa). The probability of occurrence of an event sequence caused by failure or unacceptable performance of the individual SSC ITS is estimated by convolving (or integrating) the mean seismic hazard curve with the mean fragility curve. The mean fragility curve is typically described by a lognormal distribution that is defined by the median capacity and the composite logarithmic standard deviation. The fragility and the hazard curves are convolved either by closed form solution or numerical integration. This report describes methodologies to estimate the fragility parameters, and the effects of sensitivity of these parameters on calculating the probability of unacceptable performance of SSCs ITS.

CONTENTS

FIGURES

TABLES

ACKNOWLEDGMENTS

This report was prepared to document work performed by the Center for Nuclear Waste Regulatory Analyses (CNWRA®) for the U.S. Nuclear Regulatory Commission (NRC) under Contract No. NRC–HQ–12–C–02–0089. The activities reported here were performed on behalf of the NRC Office of Nuclear Material Safety and Safeguards, Division of Spent Fuel Management. This report is an independent product of the CNWRA and does not necessarily reflect the views or regulatory position of the NRC.

The author thanks J. Stamatakos and O. Pensado for reviews and L. Neill for document preparation support.

QUALITY OF DATA, ANALYSES, AND CODE DEVELOPMENT

DATA: All CNWRA-generated data contained in this report meet quality assurance requirements described in the CNWRA Quality Assurance Manual. Sources of other data should be consulted for determining the level of quality of those data. No original data were generated in this report.

ANALYSES AND CODES: Microsoft® Excel® 2010 was used for the calculations and plots reported in this document.

1 INTRODUCTION

1.1 Background

The proposed geologic repository at Yucca Mountain would be designed to handle 70,000 metric tons of heavy metal (MTHM) of high-level radioactive wastes for permanent disposal underground. During the preclosure period, defined as the period before permanent closure of the repository, the geologic repository operations area (GROA) will receive spent nuclear fuel and high-level waste, which through a series of remote operations in the surface facilities will be repackaged, aged, transported, and finally emplaced in the underground repository. The U.S. Department of Energy (DOE) considered seismic hazards as credible natural hazards at the Yucca Mountain site (DOE, 2007) and developed methodologies for repository seismic design and demonstration of preclosure safety for seismically initiated events.

DOE topical report YMP/TR-003 (DOE, 2007) described methodologies and criteria for seismic design of structures, systems, and components (SSCs) that are important to safety (ITS). DOE established seismic design basis ground motions for SSCs based on radiological consequences (DOE, 2007). DOE assigned design basis ground motion (DBGM)-2 to SSCs ITS, which if failed, could result in radioactive releases exceeding Category 2 event sequence dose limits, which is 5 rem total effective dose equivalent (TEDE) at or beyond the site boundary. The DBGM-2 ground motion was established by DOE with a mean annual probability of exceedance (MAPE) equal to 5×10^{-4}. The DBGM-2 SSCs are designed using the procedures and acceptance criteria of NUREG-0800 (NRC, 2007a) and provisions of the codes and standards therein. The SSCs designed to the codes and standards exhibit linear elastic behavior. DOE established a beyond design basis ground motion (BDBGM) with a MAPE equal to 1×10^{-4}. The SSCs designed to DBGM-2 are evaluated for BDBGM so that the strength capacity is not exceeded by this seismic demand.

1.2 GROA Facility and Operations

The GROA surface and subsurface facilities are located in the North Portal area of Yucca Mountain, Nevada. The DOE surface facility design envisioned several building structures where radioactive waste would be handled and repackaged, and an aging facility where radioactive waste and spent nuclear fuel would cool down to acceptable thermal conditions on surface aging pads prior to emplacement underground. For all these operations, the DOE surface facilities design includes aging pads, specialized transporters, wet handling facilities, and canister transfer facilities.

The DOE design proposed surface structures containing concrete shear walls, diaphragm slabs, and mat foundations. Some buildings may also include braced-frame steel structural systems. The automated operations are supported by mechanical, electrical, and instrumentation and control systems. Several types of mechanical equipment are used in loading, unloading, and transferring transportation casks, canisters, waste packages, and spent fuel assemblies. Typical mechanical systems used in these operations are cask handling cranes, canister transfer machines, cask transfer trolleys, spent fuel transfer machines, waste package transfer trolleys, site transporters, and transport and emplacement vehicles. Other systems used in the facility are heating ventilation air conditioning systems, electrical cabinets (containing relays), piping systems, roll-up doors, and shield doors. All these SSCs ITS were designed by DOE to

perform their intended safety functions in order to prevent or mitigate any adverse consequences from a design basis or beyond design basis initiating seismic event.

1.3 Potential Seismic Risks at GROA

Understanding of seismic risks under risk-informed performance-based regulation is predicated on an accurate description of the risk triplet: what can go wrong?; how likely is it?; and what are the potential consequences? The key elements of seismic risk assessment are seismic hazard analyses, fragility evaluations, and event sequence analyses. The seismic hazard at a site is defined by a hazard curve, which describes the annual probability of exceeding seismic ground motion levels. The ground motion in a hazard curve is typically defined by peak ground acceleration, or by a range of spectral accelerations (usually between 100 and 1 Hz). The fragility of an SSC is defined by a fragility curve, which is the conditional probability of failure of the SSC for a range of seismic ground motions. The fragility curves are developed considering the uncertainties in the demand (seismic response) and capacity parameters for a specific failure mode of the SSC and the ground motions in the fragility evaluation is either peak ground acceleration or spectral acceleration consistent with the hazard curve. Event sequence analysis includes identification of seismically induced initiating events and postulated failure of one or more SSCs, intended to prevent or mitigate adverse radiological consequences.

In a repository facility, the initiating events may be caused by seismically induced failure of equipment (e.g., a damaged crane) impacting waste containers leading to the potential loss of containment or breach of the waste container upon impact and loss of confinement from failures of concrete building structures or heating, ventilation, and air conditioning (HVAC) systems. These failures could lead to releases of radioactive material to the environment. Several outcomes or sequence of events are possible based on the success and failure of the SSCs designed to mitigate these adverse radiological consequences. Initiating event frequency can be evaluated by convolving fragility and seismic hazard curves. Sometimes it may be easier to combine the fragilities of the SSCs in each event sequence using Boolean logic to evaluate sequence level fragility and then convolving with hazard curves to evaluate event sequence frequency. The outcome of each event sequence also determines potential conditions for dose consequences based on mitigated, unmitigated, or even no release of radioactive material. Approaches to demonstrate compliance with 10 CFR Part 63 for seismically initiated event sequences are discussed in Chapter 2 of this report.

1.4 Objective

The objective of this report is to document (i) the NRC information collected on seismic fragility and performance and (ii) prelicensing activities NRC performed to assist preparations for review of DOE seismic event sequences. This report discusses the review methodology developed in HLWRS-ISG-01 (NRC, 2006) in Chapter 2, the approaches to evaluate fragility of SSCs in Chapter 3, and sensitivity analyses in Chapter 4. Information presented in this report may be of interest to other safety analyses and reviews involving seismic hazards.

2 REVIEW METHODOLOGY OF SEISMIC EVENT SEQUENCES

The review methodology in ISG HLWRS–ISG–01 (NRC, 2006) is based on evaluating event sequences for seismically initiated events. The basic elements of the methodology are depicted in the flow chart shown in Figure 2-1. The ISG assumes that the site has been adequately characterized and a suitable seismic hazard curve has been developed. The ISG also assumes that the design information of the SSCs are available to compute the probability of failure (i.e., fragility as a function of ground motion). .

An event sequence, as defined in 10 CFR Part 63, includes an initiating event and the associated combinations of repository system component failure-subordinate events. The event sequence is usually represented by an event tree. Each branch of the tree represents an event sequence and its frequency of occurrence calculated from the combination of failure probabilities of SSCs and initiating event frequency. Each branch also represents the outcome in terms of potential consequences.

The methodology described herein is based on evaluating event sequences for seismically initiated events and identifying SSCs ITS for seismic performance evaluation. The first step in estimating the probability of occurrence of seismic event sequences is to assess the seismic performance of the individual SSC ITS. To obtain the mean fragility curve of the individual SSC ITS, the median capacity ($C_{50\%}$) and the composite logarithmic standard deviation (β_C) are to be estimated using a transparent technical basis. Failure criteria used for estimating the fragility curves are to be consistent with the SSCs ITS functional requirements.

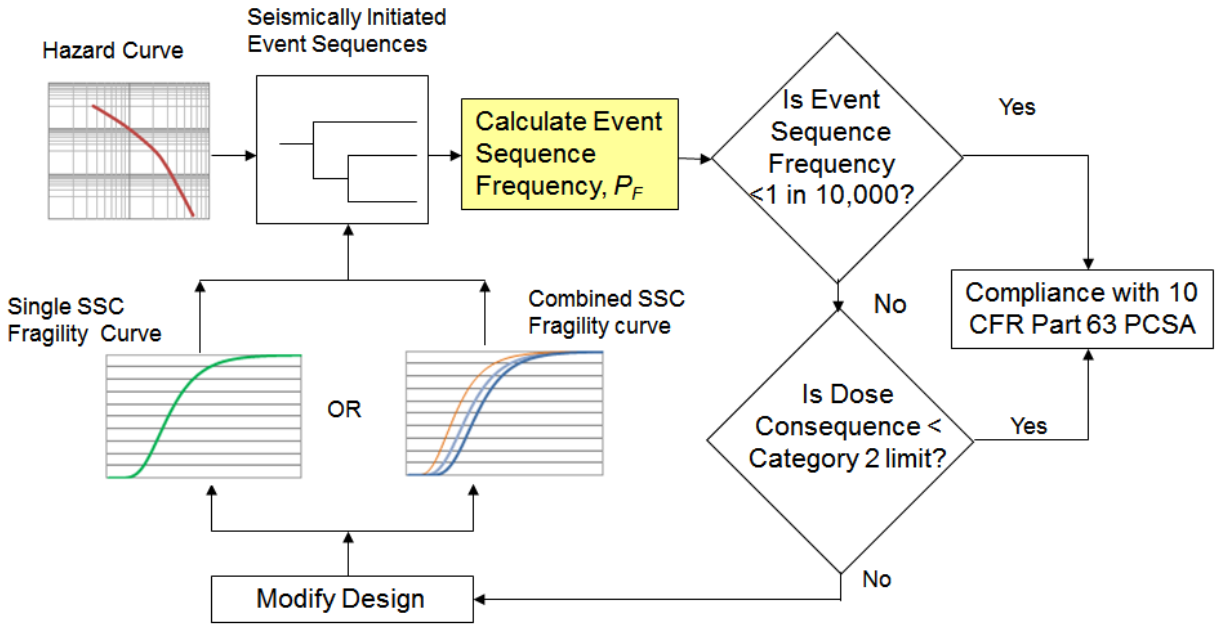

Figure 2-1: Overview of approach for seismic event sequences for compliance with 10 CFR Part 63 preclosure safety analysis

The probability of occurrence of an event sequence, P_F, caused by failure or unacceptable performance of the individual SSC ITS, is estimated by convolving (or integrating) the mean seismic hazard curve with the mean fragility curve. If the probability of failure values of

individual SSCs ITS for seismically initiated event sequences is less than 1 in 10,000 during the preclosure period for Category 2 event sequences, the SSC ITS is considered to perform its intended safety function and thereby meet the performance objectives in 10 CFR 63.111. If the preclosure period is assumed to be 100 years, the annual probability of failure limit for Category 2 event sequences is defined as 10^{-6}.

If, however, the probability of failure of the individual SSCs ITS for seismically initiated event sequences is greater than or equal to 1 in 10,000 during the preclosure period, compliance with 10 CFR 63.111 can be met by showing that the probability of occurrence of each of the seismic event sequences containing the SSC ITS is less than 1 in 10,000 during the preclosure period. In other words, that the likelihood of the subordinated events in the event sequence in combination with the initiating event are sufficiently low such that the full event sequence has a probability of less than 1 in 10,000 during the preclosure period. Note that as an alternative, regulatory compliance can also be met by showing that the dose consequence to the public at the site boundary from the event sequence is less than the dose limits in 10 CFR 63.111(b)(2). DOE's approach in their Yucca Mountain Safety Analysis Report, however, is to demonstrate preclosure safety for seismically initiating events by showing that the probability of occurrence of each event sequence is below the Category 2 limit.

The approaches for estimating the mean fragility curve for an SSC ITS, as stated in the ISG, may be based on: (i) probability density functions for controlling parameters in a Monte Carlo analysis; (ii) simplified methods outlined in Section 4 of Electric Power Research Institute (EPRI) TR-103959 (EPRI, 1994); or (iii) other methods that capture appropriate variability and uncertainty in parameters used to estimate the capacity of the SSCs ITS to withstand seismic demands. An estimate of fragility for an SSC may be based on fragility values for an identical or similar component, as found in the literature, provided technical bases for the relevance of the data to the SSC under consideration are established.

The methodology described in the ISG to evaluate seismic performance of an SSC ITS is similar to the one outlined in the American Society of Civil Engineers (ASCE)/SEI 43-05 (ASCE, 2005).

2.1 Seismic Performance

The seismic performance or probability of failure of an SSC ITS, P_F, is estimated by convolving the site specific seismic hazard curve and fragility curve of the structure. The seismic hazard curve $H(a)$ is the annual probability of exceedance of ground motion level (a), which is defined by peak ground acceleration or spectral acceleration. The fragility curve of the structure $P_{f/a}$ is the conditional cumulative probability of unacceptable performance and can be defined by the median capacity $C_{50\%}$ and the composite logarithmic standard deviation β_c. Then P_F can be estimated as ASCE, 2005; (Kennedy, 1999a,b):

$$P_F = -\int_0^\infty P_{f/a}\left(\frac{dH(a)}{da}\right)da \tag{2-1}$$

or

$$P_F = \int_0^\infty H(a)\left(\frac{dP_{f/a}}{da}\right)da \tag{2-2}$$

The convolution can be performed numerically or by using a closed-form solution.

2.1.1 Closed-Form Expression

The seismic hazard curve is assumed to be linear when plotted in log–log scale and approximated by a power law as (ASCE, 2005; Kennedy, 1999a)

$$H(a) = K_1 a^{-K_H} \tag{2-3}$$

Where K_H is the slope parameter given by $K_H = 1/\log(A_R)$. The parameter A_R is the ratio of the spectral acceleration, Sa, corresponding to a 10-fold reduction in exceedance frequency and given by the following equation

$$A_R = \frac{Sa_{0.1H_D}}{Sa_{H_D}} \tag{2-4}$$

where

Sa_{H_D} = Spectral acceleration at exceedance frequency, H_D

$Sa_{0.1H_D}$ = Spectral acceleration at exceedance frequency, $0.1H_D$

The parameter K_1 is a constant obtained by using Eq. 2-3 after K_H is computed.

Approximating the hazard curve as given in Eq. (2-3) and considering the fragility to be lognormally distributed and defined by $C_{50\%}$ and β_c, the closed form solution is given as (ASCE 2005, Kennedy 1999b; McGuire, 2004):

$$P_F = K_1 (C_{50\%})^{-K_H} \; e^{0.5(K_H \beta_c)^2} \tag{2-5}$$

2.1.2 Numerical Integration

In this study, P_F was obtained using numerical integration, in which the hazard curve is discretized into equal intervals and assumed to be a piecewise linear. The value for P_F is obtained by summing the products of the hazard exceedance and the fragility values at each ground motion interval (Kennedy and Short, 1994). The annual probability of failure P_F is given by the following equation

$$P_F = \sum_{i=1}^{n} [H(a_i) - H(a_{i+1})] P_{F/a_{cgi}} \tag{2-6}$$

where, $P_{F/a_{cgi}}$ is the conditional failure probability at ground motion level a_{cgi}, which is the acceleration at the center-of-gravity point of the hazard curve between a_i and a_{i+1} accelerations, and n is the number of discretization of the of the hazard curve.

2.1.3 Example Methodology for Evaluation of Complete Event Sequence

HLWRS-ISG-01 presented an example to evaluate the probability of occurrence of seismically induced event sequences. The example is based on conceptualized canister handling

operations. Hypothetical seismic hazard curve and fragility curves of structures and equipment were used in the example. The evaluation is typically performed at appropriate frequencies based on dynamic characteristics of SSC ITS. The example evaluation is performed at 10 hertz (Hz) structural frequency.

The conceptualized facility operations, as shown in Figure 2-2, include transfer of canister from transportation cask to a waste package. The facility structure is assumed to consist of concrete shear walls, and floor and roof slabs constructed on a concrete mat foundation. The canister is transferred using a bridge crane. The HVAC and High Efficiency Particulate Air (HEPA) system provide filtration of potential release radionuclide particles in the transfer cell.

The hypothetical seismic hazard curve at 10 Hz, $H(a)$, and annual probability of exceedance as a function of spectral acceleration is shown in Figure 2-3. The mean fragility curve of an SSC ITS for a defined failure mode is expressed in terms of a median capacity, $C_{50\%}$, and composite logarithmic standard deviation, β. The fragility parameters for the SSCs in this example are given in Table 2-1.

P_F, for individual SSCs ITS

The annual probabilities of failure, P_F, for individual SSCs ITS are estimated and given in Table 2-1. Based on this example analysis, the crane components, concrete shear wall, and HVAC duct anchor system each have probabilities of failure greater than 1 in 10,000 during the preclosure period or an annual probability of 10^{-6} for a Category 2 event sequence, assuming a 100-year preclosure period. Therefore, this example event sequences needs to be evaluated further.

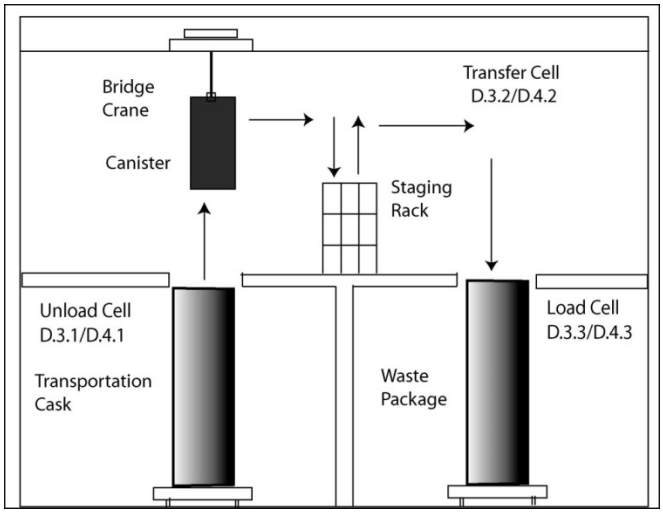

Figure 2-2. Conceptual waste handling operations

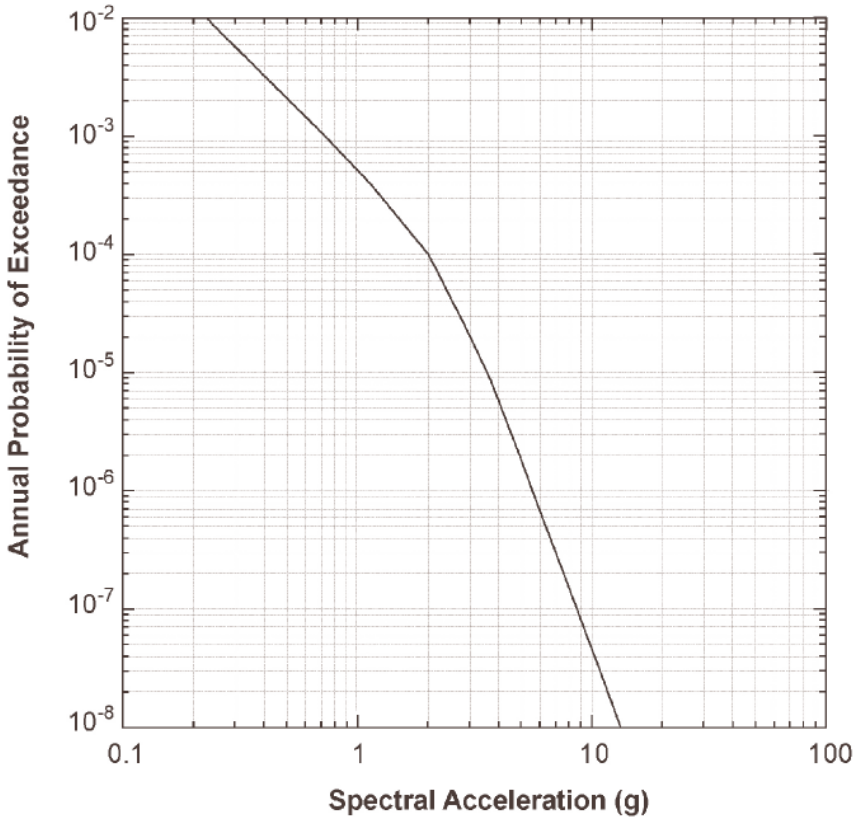

Figure 2-3. Hypothetical seismic hazard curve used in the example analysis

Table 2-1. Assumed fragility parameters of SSC ITS at 10 Hz structural frequency and the annual P_F			
SSC ITS	$C_{50\%}$	β	P_F
Crane System	6.3g	0.4	3.2×10^{-6}
Concrete Shear Wall	7.2g	0.35	1.2×10^{-6}
HVAC Duct Anchor System	5.7g	0.45	6.7×10^{-6}
g: acceleration due to gravity $C_{50\%}$: median capacity β : composite logarithmic standard deviation P_F : Annual probability of failure or probability of unacceptable performance			

Sequence of Events

A potential sequence of events in this example, depicted in an event tree shown in Figure 2-4, is as follows:

- Failure of components in the crane system during a seismic event while canister transfer operation drops the canister and initiates the seismic event sequences (top event CRN_COMP)

- Canister failure from the drop is assumed not to perform its intended safety function (loss of containment) resulting in release of radionuclide material inside the facility: probability of loss of containment, given a drop is assumed as 1.0 (top event CANIS_BRCH)

- Failure of concrete shear wall during the seismic event, may result in loss of confinement (top event STR_SHWL)

- Failure of HVAC duct anchor system during the seismic event may result in loss of confinement (top event HVAC_ANC)

End-state of the event sequences

The end-state of the event sequences as shown in Figure 2-2 are as follows:

Initiating Event: Crane system fails and drops the canister

Event Sequence 1: No radionuclide release because canister integrity on success path (i.e., no loss of containment).

Event Sequence 2*:* Mitigated release may occur if the canister fails (breach) from drop. However, because both structural shear wall and HVAC system are on the success paths, the radiological release to the environment is filtered through a HEPA. The annual probability of occurrence of the event sequence is the same as the annual probability of unacceptable performance of the crane, P_F, which is 3.2×10^{-6}, as shown in Table 2-2. Frequency of the event sequence is greater than 10^{-6} for a Category 2 event sequence, assuming a 100-year preclosure period. Thus, demonstration of compliance with Category 2 dose consequence would be required.

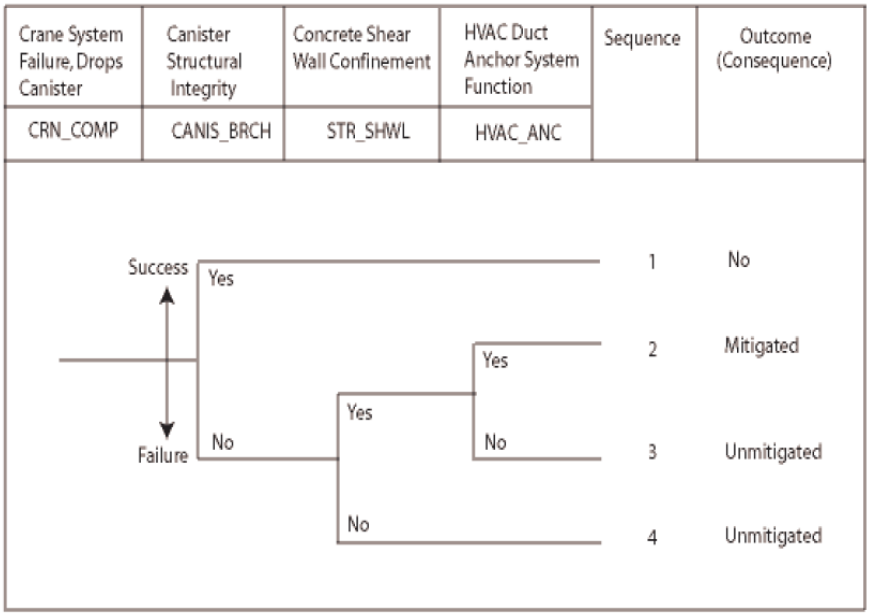

Figure 2-4. Seismically initiated event sequences

Table 2.2. Description of outcome of each event sequence				
Event Sequence	**Fragility of Components**	**Event Sequence Frequency**	**Potential Outcome**	**Compliance of Event Sequences with Regulatory Performance Objectives**
2	Crane System	3.2×10^{-6}	Mitigated release	Frequency greater than Category 2 frequency limits, demonstration of compliance with Category 2 dose consequence required
3	Crane System and HVAC Anchor System	8.4×10^{-7}	Unmitigated release	Frequency less than Category 2 frequency limits, dose consequence evaluation not required
4	Crane System and Shear Wall	3.8×10^{-7}	Unmitigated release	Frequency less than Category 2 frequency limits, dose consequence evaluation not required

Event Sequence 3: Unmitigated release may occur if canister fails (breach) from drop and HVAC duct anchor system supporting the duct fails; however, structural shear wall is on success path. For simplicity, it is assumed, in this example, that if the HVAC duct anchor system fails, all the radioactive materials released to the environment because of the potential canister breach would be discharged through the HVAC system.

In this event sequence, the fragilities of the crane system and the HVAC duct anchor system are dependent on the spectral acceleration of the seismic event. However, the fragilities of these two systems are independent of each other. Therefore, the combined fragility of the two systems in the event sequence can be obtained by multiplying fragilities of each system at various seismic spectral acceleration values. The fragility curve for the event sequence was obtained, as shown in Figure 2-5(a). To determine the probability of occurrence of the event sequence, the combined fragility curves for both SSCs ITS must then be convolved with the hazard curve. The annual probability of occurrence of the event sequence of 8.4×10^{-7} is less than 10^{-6} (assuming a 100-year preclosure period) demonstrating compliance with Category 2 event sequence.

Event Sequence 4*:* Unmitigated release may occur if the canister fails from the drop and the concrete shear wall fails to confine radioactive material. In this event sequence, the fragilities of the crane system and the concrete shear wall can be combined. See Figure 2-5(b) for example fragility curves of the SSCs ITS in this event sequence. The resulting annual probability of occurrence of the event sequence is 3.8×10^{-7}, which is less than 10^{-6} (assuming a 100-year preclosure period) demonstrating compliance with Category 2 event sequence.

Although evaluation of individual SSC ITS in an event sequence may indicate a probability of failure of greater than 10^{-6} during a seismic event, this example shows that appropriate consideration of these SSCs ITS jointly may result in an event sequence probability of occurrence that is less than 10^{-6}, which is not a credible event sequence for the preclosure safety analysis. If the event sequence annual probability of occurrence were greater than 10^{-6}, it would be considered a Category 2 event sequence. In this case, a radiological consequence

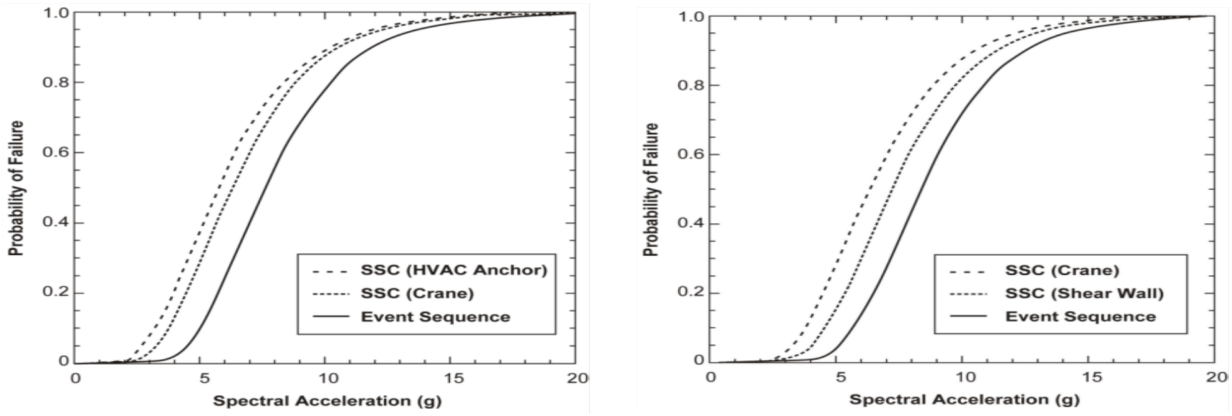

(a) (b)

Figure 2-5. Hypothetical fragility curves used in the example analysis. Individual and combined fragility for: (a) event sequence 3 and (b) event sequence 4

assessment would be needed to demonstrate that the numerical dose limits of 10 CFR 63.111(b)(2) are not exceeded.

Key Messages

- Seismic performance of SSCs ITS may be determined using a methodology outlined in the ASCE Standard ASCE 43-05 (ASCE, 2005).

- Seismic hazard for the preclosure safety analysis should be characterized using an appropriate site response model and to low-enough values of annual probabilities of exceedance so that its combination with fragilities of SSCs ITS appropriately supports estimates of event sequence probabilities of occurrence.

- Fragility curves for SSCs ITS should be developed using transparent technical bases and the failure criteria consistent with the SSCs ITS functional requirements.

- If more than one SSC ITS are relied on for categorizing an event sequence, individual SSCs fragility curves may be combined to determine the event sequence probability of occurrence.

3 METHODOLOGY FOR FRAGILITY CURVE EVALUATION

As stated in HLWRS-ISG-01, the mean fragility curve for SSCs ITS may be estimated using methods that capture appropriate variability and uncertainty in parameters used to estimate the capacity of the SSCs ITS to withstand seismic events. In addition, the ISG stated that an estimate of fragility for an SSC may be based on fragility values for an identical or similar component, as found in the literature, provided appropriate technical bases are established. In this section, the methodologies used in the developing seismic fragility curves are discussed and the fragility data from past seismic probabilistic risk assessment of nuclear power plants are reviewed. NRC also developed ISG HLWRS-ISG-02 (NRC, 2007b) as guidance to the staff for reviewing the reliability of passive components. This ISG may be relevant should DOE rely on the passive components for preventing or mitigating seismic event sequences.

3.1 Fragility Curve

Seismic fragility of a structure or equipment is defined as the conditional probability of failure for a given level of seismic ground motion. Typically, the ground motion is defined as the peak ground acceleration (PGA) or spectral acceleration (Sa) at frequencies consistent with the ground motion parameter used to define the site specific seismic hazard curve. The objective of fragility evaluation to estimate the ground motion level at which the seismic response of a given component exceeds the component capacity resulting in failure (unacceptable performance). The component fragility is defined as a family of fragility curves capturing many sources of variability in the parameters for estimating seismic response (demand) and capacity.

The fragility curve is typically depicted by a lognormal distribution that is defined by the median capacity, $C_{50\%}$, and the logarithmic standard deviation, which may be separated into epistemic uncertainty, β_U, and random variability, β_R. The median capacity, $C_{50\%}$, is the ground motion at which the component has 50 percent chance of failure. The epistemic uncertainty (β_U) is the uncertainty range of the median capacity and defines the spread or width of the confidence bands of the fragility curve, whereas the random variability (β_R) defines the shape of the curve (EPRI, 1994; Kennedy, 1999a). A family of fragility curves shown in Figure 3-1 is typically represented by 95-, 50-, and 5-percent confidence levels.

The mean fragility curve is a single curve defined by median capacity, $C_{50\%}$, and composite logarithmic standard deviation β_C. The epistemic uncertainty and random variability can be replaced by a composite or total variability (Kennedy, 1999b), β_C, given as:

$$\beta_C = \sqrt{\beta_U^2 + \beta_R^2} \tag{3-1}$$

As shown in Figure 3-1, the ground motion level at which there is approximately 95 percent confidence of less than or about 5 percent probability of failure is defined as HCLPF. HCLPF capacity also corresponds to approximately 1 percent probability of failure ($C_{1\%}$) on the mean (composite) fragility curve.

Once a mean fragility curve is defined, C_{HCLPF} can be computed from the following equation:

$$C_{HCLPF} = C_{1\%} = C_{50\%} e^{-2.326\beta_C} \tag{3-2}$$

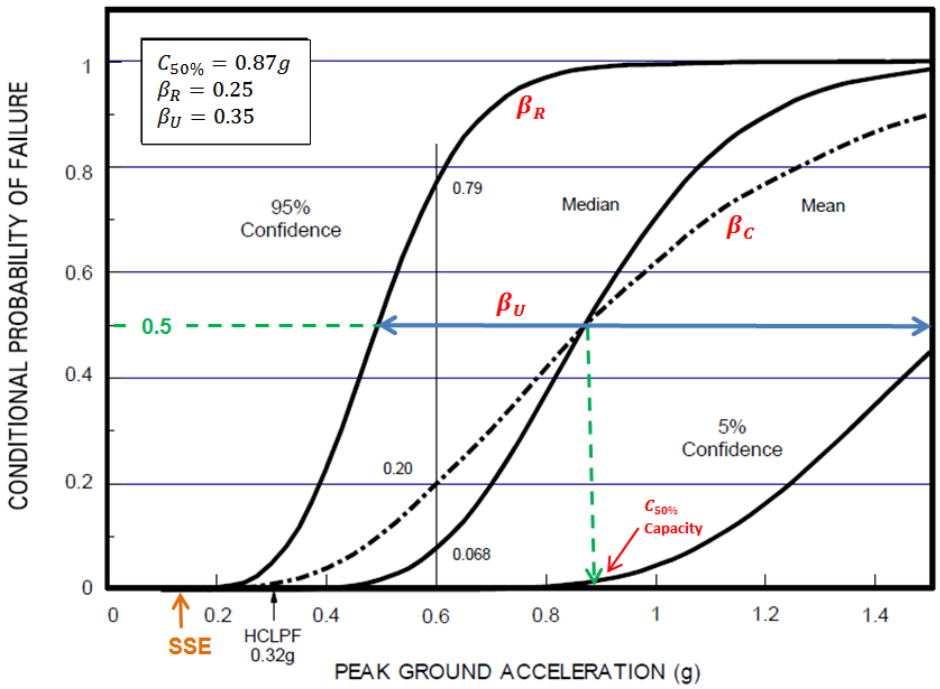

Figure 3-1. Example showing mean, median, 5 percent, and 95 percent nonexceedance fragility curves for a component including design earthquake (SSE) $C_{50\%}$, and HCLPF capacity points.

3.2 Estimation of Fragility Parameters

The flow chart for fragility evaluation for structural components and subsystems (e.g., equipment located inside the structure at floor levels) is shown in Figure 3-2. The fragility evaluation includes estimation of seismic demand on the structures from response analysis and the capacity of the structural systems and equipment to withstand the demand. Seismic response involves dynamic modeling of ITS surface facility structures for the site specific ground motion. The proposed waste handling facilities are primarily reinforced concrete structural systems consisting of shear wall, floor slabs, and mat foundation, including steel framing in some facilities. Since the structures will be founded on thick alluvium overlaying the bedrock soil-structure, interaction analysis is needed for evaluating dynamic response of the structures. For structural dynamic analysis of nuclear facility structures, typically three-dimensional lumped-mass-stick model or finite element models are used to calculate the demand (e.g., bending moment, shear force, axial force) on the structural elements. In addition, overall structural response (e.g., potential sliding of foundation, structural deformation or story drift, floor acceleration) are obtained from the response analysis. Floor acceleration is used to develop in-structure response spectra for response modeling of individual equipment and estimating demand forces.

Fragility curves of components are then developed for a given failure mode. The first step for developing fragility curves is to define modes of structural failure induced by seismic loading. Examples of failure modes for concrete and steel structural systems are given in Table 3-1. As can be seen in Table 3-1, there are three potential failures for a shear wall: diagonal shear cracking, flexure, and shear friction. All failure modes must be investigated and the fragility of the wall is estimated based on the lowest capacity of the three failure modes. In nuclear

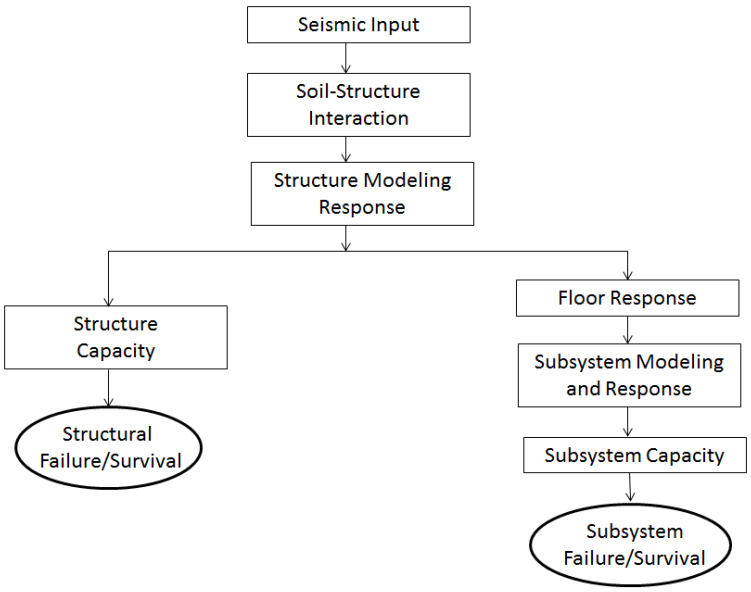

Figure 3-2. Fragility analysis flow chart

Table 3-1. Example failure modes of components in potential repository	
Components	**Failure modes**
Civil Structures	
Reinforced Concrete Structures	Shear Wall — Plane shear failure of Shear Walls — Out-of-plane bending failure — Shear friction Diaphragm slabs
Steel Structures	Flexure and shear failure of Steel girders Buckling failure of Columns Tensile and bucking failure of frame components
Equipment	
Bridge Crane, Canister Transfer Machine	Collapse of bridge girders Load drop due of failure of hoist, drum
Trolley, site transporter	Tipover
Platform, support frame, staging rack	Collapse
Transport Emplacement Vehicle	Tipover Derailment Ejection of Waste package
Piping System	Rupture
HVAC System	Duct anchor failure

facilities, the shear walls contain several openings. The three failure modes are considered to determine the lowest capacity for each pier and the sum of pier strengths determines the wall capacity. Examples of failure modes for equipment, likely to be used at a repository, also are given in Table 3-1. Equipment and component failure mode include anchorage, functional failures, and failure due to seismic interactions.

Each failure mode is associated with a predefined limit state or limiting acceptable condition of the SSC. In other words, if the limiting condition is exceeded, the performance of structural or equipment is considered to be unacceptable or failed. ASCE (2005) defined four limit states (A through D) for structural systems, which varies from elastic deformation (no damage) to short of collapse, as shown in Table 3-2. The limit state may be defined in terms of maximum acceptable displacement, strain, ductility, or stress (ASCE, 2005). The limit state for structural systems is defined in terms of total drift ratio for each story. The drift ratio is the story deflection divided by the story height. Allowable drift ratio limits for reinforced concrete shear wall, for example, are shown in Table 3-2. In fragility analysis, the failure modes and the limit states should be consistent with the SSC ITS functional requirements credited in the safety analysis.

Fragility evaluation should capture appropriate variability and uncertainty in parameters used to estimate the capacity of the SSCs. For $\beta_{R,}$ sources of variability cannot be reduced by more detailed studies or more data. The example includes inherent variability in earthquakes that cause randomness in structural response. For $\beta_{U,}$ sources of variability are due to lack of knowledge of structural response and uncertainties in the capacity can be reduced by detailed studies or more data. Examples include uncertainties in dynamic modeling of structures, lack of understanding of material capacity, etc.

The two approaches commonly used in developing mean fragility curves: (i) conservative deterministic failure margin (CDFM) method and (ii) separation of variable are discussed next.

Table 3-2. Limit state, allowable drift limits, and inelastic absorption factor for shear controlled walls, $h_w/l_w < 2.0$*

Limit State	Structural Deformation Limit	Amount of Damage	Allowable Limit, Drift Ratio†	Inelastic absorption factor, F_μ‡
A	Large permanent distortion, short of collapse	Significant	0.0075	2.0
B	Moderate permanent distortion	Generally repairable	0.006	1.75
C	Limited permanent distortion	Minimal	0.004	1.5
D	Essentially elastic behavior	None	0.004	1.0

* h_w =height and l_w = length of shear wall
†ASCE (2005) Table 5-2
‡ASCE (2005) Table 5-1

ASCE, American Society of Civil Engineers, Structural Engineering Institute. "Seismic Design Criteria for Structures, Systems, and Components in Nuclear Facilities." ASCE/SEI 43-05. Reston, Virginia: American Society of Civil Engineers, Structural Engineering Institute. 2005.

3.2.1 Fragility Curve using CDFM method

The approach to develop a mean or composite fragility curve using CDFM is discussed in (Kennedy, 1999b; EPRI, 1991). In this methodology, the median capacity, $C_{50\%}$, is obtained from the capacity estimated at $C_{1\%}$ and the logarithmic standard deviation, β_C is assumed

based on judgement. Using the lognormal property, $C_{50\%}$ can be estimated from $C_{1\%}$ by the following equation:

$$C_{50\%} = C_{1\%} e^{2.326\beta_C} \tag{3-3}$$

Kennedy (1999b) showed that HCLPF capacity computed by the CDFM method closely approximates $C_{1\%}$ on the mean fragility curve (see Eq. 4-2). Thus, C_{HCLPF}, and $C_{1\%}$, and CDFM capacity are synonymous. As described in NUREG–1407 (NRC, 1991), the NRC staff accepted the CDFM method as an approximate method for estimating C_{HCLPF}. In this method, the β_R and β_U are not estimated separately; instead, β_C can be assumed from a range of values recommended by ASCE (2005) for structures and equipment. Kennedy (1999b) called this approach the Hybrid Method, which uses a simpler deterministic method of the Seismic Margin Assessment approach to develop fragility curves and uses the Seismic Probabilistic Risk Assessment approach for convolving fragility and seismic hazards curves for estimating either individual SSC annual probability of unacceptable performance or event sequence frequency.

The HCLPF capacity of any structural element is the ground motion level above a reference ground motion. Using the CDFM approach, the HCLPF capacity is given by the following equation:

$$C_{HCLPF} = F_S \cdot F_\mu \cdot PGA_{Ref} \tag{3-4}$$

where,

PGA_{Ref} = reference level earthquake
F_S = strength margin factor
F_μ = inelastic energy dissipation factor

PGA_{Ref} is the peak ground acceleration of the reference earthquake level at which the plant margin is evaluated. The reference earthquake is typically set at ground motion higher than design basis earthquake. For example, for surface facility structures at Yucca Mountain, DOE used earthquake (DMGM-2) at Mean Annual Probability of Exceedance (MAPE) 5×10^{-4} and used a BDBGM with a MAPE equal to 1×10^{-4} as the reference earthquake.

The strength margin factor, F_S, for an individual element is given by

$$F_S = \frac{C - D_{NS}}{D_{Refeq}} \tag{3-5}$$

where,

C = element capacity computed using code capacity acceptance criteria
D_{NS} = expected concurrent non-seismic demand.
D_{Refeq} = seismic demand computed at reference earthquake

In the CDFM method, the demand and capacity are evaluated using the best estimate parameters and code specified values. The dynamic input for the response analysis is a smooth response spectra based on Uniform Hazard Spectra (UHS) obtained from Probabilistic Seismic Hazard Analysis PSHA (EPRI, 2009) and consistent with the MAPE of the reference earthquake. The seismic demand forces, D_{Refeq}, are obtained from structural seismic

analysis results. Seismic demand should be computed in accordance with NRC guidance (NRC, 2007a) and ASCE standards (1998 and 2005). The seismic demand is computed using linear equivalent static analysis, linear dynamic analysis, or non-linear dynamic analysis. Considerations for the structural response analysis include static and dynamic loading (ground motion), structural model (e.g., lumped-mass stick model, finite element method), material damping, and soil-structure interaction, as discussed in ASCE (2005, 1998).

Relevant codes and standards used for structural static capacity, C, of reinforced concrete and structural steel components are given in ASCE (2005). For reinforced concrete wall structures ASCE (2005) specifies that the design shall be based on strength design method. The nominal capacity of the concrete structures are calculated using American Concrete Institute (ACI)-349, except for the low-rise shear walls (height/length < 2.0), where the capacity given in ASCE (2005) is recommended. For structural steel members the capacity is determined using provisions of American Institute of Steel Construction (AISC). The material strength used in capacity calculations should be code specified with minimum strength. If material test data are available, approximately 95 percent exceedance probability strengths can be used (EPRI, 1991).

The inelastic energy absorption accounts for additional capacity because of ductility design detailing. The inelastic energy dissipation factor F_μ for a range of the structural elements and limit states is given in ASCE (2005). An example of the F_μ factors for shear wall failing in shear failure mode is given in Table 3-2, which shows that F_μ increases from 1.0 from limit state D (elastic) to 2.0 for limit state A (near collapse). F_μ factors may be reduced to account for weak/and or soft story effects. When the structure has either a weak or a soft story determined by whether the strength or stiffness of a story is less than the above story, the F_μ factor is reduced in accordance with ASCE (2005).

The logarithmic standard deviation β_C for the mean fragility curve is assumed based on judgment from a range of values given in ASCE (2005). For structures and equipment mounted on ground level, the β_C varies between 0.3 and 0.5 and for equipment mounted high in the structure, β_C varies between 0.4 and 0.6. Kennedy (1999b) noted that overestimating β_C artificially increases $C_{50\%}$ capacity, thus, assumption of β_C should be supported by technical justification. The extent of the variation of β_C on the unacceptable performance, P_F, of the structural element is evaluated in Chapter 4 of this report.

3.2.2 Fragility Curve using Separation of Variables Approach

Evaluation of fragility parameters by the separation of variable method is summarized here based on EPRI (1994) and Kennedy and Ravindra (1984). In this methodology, the median capacity, $C_{50\%}$, including epistemic uncertainty, β_U, and random variability, β_R are estimated for structures and equipment. The mean fragility curve is developed using $C_{50\%}$ and the composite logarithmic standard deviation, β_C Eq. (3-1). The fragility parameters are calculated by considering the contributions of various capacity and demand or response parameters. The variables associated with capacity and demand for structures and equipment are given below:

- Capacity parameters
  - Strength
  - Inelastic energy absorption

- Structural response or demand parameter
  - Spectral shape (Seismic input randomness)
  - Soil structure interaction (soil stiffness, vertical spatial variation of ground motion, damping)
  - Modeling (frequency and mode shapes)
  - Damping
  - Modal combinations
  - Combination of earthquake components

- Equipment response or demand parameters
  - Modeling (frequency and mode shape)
  - Damping
  - Modal combination
  - Combination of earthquake components

In addition, the variables needed to account for the ground motion are: response spectra shape, horizontal direction peak response, and vertical component response. The detailed information can be obtained from EPRI (1994).

Structures

The median capacity, $C_{50\%}$, by separation of variable is given by (EPRI, 1994):

$$C_{50\%} = F_m \cdot D_{PGA} \tag{3-6}$$

where F_m is the median factor of safety and D_{PGA} is the peak ground acceleration of the design earthquake. The factor of safety (F) is modeled as the product of three random variables, F_S, F_μ, and F_{SR}. The strength factor, F_S is the ratio of ultimate strength of the structural member to the stress calculated for D_{PGA}. The inelastic absorption factor F_μ, also called the ductility factor, accounts for the fact that many structures are capable of absorbing substantial amounts of energy beyond yield without loss-of-function (Kennedy and Ravindra, 1984). The structural response factor F_{SR} is modeled as a product of response variables. The equations for modeling F are:

$$F = F_S \cdot F_\mu \cdot F_{SR} \tag{3-7}$$

$$F_S = \frac{V_U - V_{NS}}{V_S} \tag{3-8}$$

where, V_U = ultimate static capacity
V_{NS} = Non-seismic loading
V_S = seismic demand (design earthquake)

$$F_\mu = \left(\sqrt{2\mu - 1}\right)\varepsilon \tag{3-9}$$

where, μ = System ductility ratio, and ε = Error variable

$$F_{SR} = F_{SA} \cdot F_{\delta} \cdot F_{M} \cdot F_{MC} \cdot F_{EC} \cdot F_{SSI} \quad (3\text{-}10)$$

F_{SA} = spectral shape factor representing variability in ground motion and associated ground response spectra.

F_{δ} = damping factor representing variability in response due to difference between actual damping and design damping.

F_{M} = modeling factor accounting for any bias and uncertainty in response due to structural modeling assumptions.

F_{MC} = mode combination factors accounting for any bias and variability in response due to the method used in combining dynamic models of response.

F_{EC} = earthquake component combination factor accounting for any bias and variability in response due to the method used in combining earthquake components. Responses from three earthquake components are typically combined by the Square-Root-of-the-Sum-of-the-Squares (SRSS) method or based on the assumption that when the maximum response from one component occurs, the response from other components are 40% of the maximum (100-40-40 rule).

F_{SSI} = factor to account for the effect of soil-structure interaction, including the reduction of input motion with depth below the surface.

In addition, a ground motion incoherence factor that accounts for the fact that a travelling seismic wave does not excite a large foundation uniformly may also be included as an additional variable (EPRI, 2009).

For each variable affecting factor of safety random (β_R) and uncertainty (β_U), variabilities are separately estimated. Essentially, β_R represents variability due to randomness of the earthquake characteristics and β_U represents dispersion because of: (i) lack of understanding of the structural material properties (i.e., strength, inelastic energy absorption, and damping); and (ii) errors in calculating.

The median of F is expressed as:

$$F_m = F_{Sm} \cdot F_{\mu m} \cdot F_{SAm} \cdot F_{\delta m} \cdot F_{Mm} \cdot F_{MCm} \cdot F_{ECm} \cdot F_{SSIm} \quad (3\text{-}10)$$

The β_R and β_U are expressed as:

$$\beta_R = (\beta_{R,S}^2 + \beta_{R,\mu}^2 + \beta_{R,SA}^2 + \cdots .. + \beta_{R,SSI}^2)^{1/2} \quad (3\text{-}11)$$

$$\beta_U = (\beta_{U,S}^2 + \beta_{U,\mu}^2 + \beta_{U,SA}^2 + \cdots .. + \beta_{U,SSI}^2)^{1/2} \quad (3\text{-}12)$$

The composite logarithmic standard deviation of F can be calculated using Eq. 3-1.

The range of values of median factor of safety for each variable and corresponding ranges for β_R and β_U based on the data collected by Kennedy and Ravindra (1984) from nuclear power plant structures is given in Table 3-5.

Equipment

For equipment and other components, the factor of safety is composed of a capacity factor, F_C, a structural response factor, F_{SR} , and equipment response (relative to the structure) factor, F_{RE} (EPRI, 1994).

$$F_E = F_C \cdot F_{RE} \cdot F_{RS} \tag{3-13}$$

The capacity factor of the equipment F_C is the ratio of the acceleration level at which the equipment ceases to perform its intended function to the seismic design level. F_C is the product of F_S and F_μ. Equipment failure is classified as elastic functional failures, brittle failures, and ductile failures. Elastic functional failures involve loss of intended function while the component is stressed below its yield point. Brittle failures are those that have little or no system inelastic energy absorption capability, and ductility failures are those in which the structural system can absorb a significant amount of energy through inelastic deformation.

The equipment response factor F_{RE} is the ratio of the equipment response calculated in the design to the realistic equipment response, where both responses are calculated for floor design spectra. For equipment qualified by analysis, the variables that influence the response are: (i) qualification method (dynamic vs static analysis), (ii) spectral shape (including peak broadening and smoothening of floor response spectra), (iii) modeling, (iv) damping, (iv) combination of modal response, and (v) combination of earthquake components (EPRI, 1994). For equipment qualified by testing, the variables that influence responses are: (i) response clipping, (ii) capacity increase and demand reduction, (iii) cabinet amplification, (iv) multi-axis to single-axis conservatism, and (v) broad frequency input spectrum device capacity (EPRI, 1994).

The structural response factor, F_{RS} , is based on the response characteristics of the structure at the location of the equipment support. The variables used to generate floor response spectra for equipment design are the variable of interest. The applicable variables are: (i) spectral shape, (ii) ground motion incoherence, (iii) damping, (iv) modeling, (v) mode combination, and (vi) soil-structure interaction (EPRI, 1994).

3.3 Fragility Data

Information on the fragility of reinforced concrete structural components is available from the past seismic probabilistic risk assessments of existing U.S. nuclear power plants (NRC, 2002, 1991; Campbell, et al., 1988; Kennedy and Ravindra, 1984; Kennedy, et al., 1980; Park, et al., 1998; Pacific Gas and Electric Company, 1988). Although the search for fragility information is not exhaustive, the collected data provides an estimation of the lower and upper boundaries for the parameters that describe fragility curves.

Fragility information for nuclear power plants obtained from Campbell, et al. (1988) was originally collected as part of the NRC program on quantification of seismic margins. The information includes fragility input to seismic probabilistic risk assessments for 20 nuclear power plants in the eastern U.S. The database identifies eight power plants for which seismic probabilistic risk assessments were already completed. The authors cautioned that the information was produced at different times and sometimes for purposes different from probabilistic risk assessment analyses. Furthermore, the fragility data is not supported by information on the structural system characteristics (e.g., shear wall thickness, reinforcement), and in some cases, the failure modes are not clearly defined. Nevertheless, this document is

one of the best sources of fragility information on structural and other components available in the literature.

For non-containment structures, the database of Campbell, et al. (1988) identifies the type of structure, failure mode, and design basis earthquake (SSE) in terms of peak ground acceleration. The parameters $C_{50\%}$ and $C_{1\%}$ are also provided in terms of peak ground acceleration. The parameter $C_{1\%}$ defines the HCLPF capacity. Campbell, et al. (1988) compiled fragility data for roof collapse, diaphragm failure, shear wall with flexural failure, and shear walls failing in shear for eastern U.S. nuclear power plants. Table 3-3 shows ranges of fragility parameters rather than individual plant parameters. The shear walls exhibiting shear failure have the largest range of median capacity in terms of peak ground acceleration (0.44 to 5.8 g). The maximum value of median capacity of shear walls failing in shear (5.8 g) exceeds the maximum median capacity of shear walls with flexural failure (4.9 g). The median capacities for roof collapse (1.84 g) and diaphragm failure (2.34 g) modes are significantly lower than the wall failure modes. Shear walls with shear failure also have the largest interval for lognormal standard deviation values (from 0.26 to 0.72) compared to other structural components.

The only fragility data collected for western U.S. nuclear power plants was obtained from the seismic risk assessment of Diablo Canyon Nuclear Power Plant (Pacific Gas and Electric Company, 1988). Regions west of the Rockies are considered to be in the high seismic region and nuclear structures are designed to handle higher ground motion than the eastern U.S. nuclear power plants. The fragility data for reinforced concrete shear wall structures of Diablo Canyon Nuclear Power Plant are summarized in Table 3-4. The table includes the type of failure mode and fragility parameters $C_{50\%}$, β_r and β_u. The composite logarithmic standard deviation of the data β_c is added to the initial data. The median capacities were evaluated in terms of 5 percent damped spectral acceleration averaged over the 3.0–8.5 Hz frequency interval. The structural information is available only for Wall 31 of the facility, which is 55 ft [16.8 m] high, 137 ft [41.8 m] long, and 2 ft [0.6 m] thick. For this western U.S. nuclear power plant, the median capacity, expressed in terms of spectral acceleration, varies from 4.87 to 8.55 g, whereas the composite lognormal standard deviation ranges from 0.33 to 0.42. Direct comparison with the data obtained with eastern U.S. nuclear power plants is not possible because the fragility data is defined in terms of peak ground acceleration for the eastern U.S. and spectral acceleration for Diablo Canyon power plant.

Kennedy and Ravindra (1984) collected data on the fragility of a wide range of structures, including concrete shear walls, from the nuclear power plants and presented median factors of safety and variability of capacity and demand parameters that relate to separation of variable approach. The data presented does not distinguish between eastern and western U.S. nuclear power plants. Table 3-5 shows the range of median factors of each contributing variable for the structural capacity and demand (i.e., ultimate strength, ductility, spectral shape, soil-structure interaction, damping, modeling effects, and mode combinations). The total median margin (factor of safety, F_m) over the design ground motion ranges from 4.0 to 12.0 for the structures designed by applicable codes and standards. Kennedy and Ravindra (1984) observed that most of the margin resulted from the conservative approach used in the capacity evaluation and to a lesser extent from the response evaluation. To account for the fragility data uncertainty, Kennedy and Ravindra (1984) obtained a range of values for randomness, β_R and uncertainty, β_U and presented in Table 3-5. The median capacity $C_{50\%}$ is estimated using Eq. 3-6, where range of F_m is given in Table 3-5 and D_{PGA} is the design earthquake. The median capacity of structural elements in Table 3-3 can be estimated using Eq. 3-6. For example, using the range (0.10–0.40g) of design ground motions (D_{PGA}) in Table 3-3 and the range (4.0–12.0) of median

factor of safety (F_m) in Table 3-5, the estimated range of median capacity is 0.4–4.8g. The ranges of median capacity for shear walls with shear and flexure failure modes from collected data in Table 3-3 are similar to the calculated range using F_m from Table 3-5.

Table 3-3. Collected fragility parameter data ranges for eastern U.S. nuclear power plants*

Structural Element	Ground Motion Parameter	DE† (g)	$C_{1\%}$ (g)	$C_{50\%}$ (g)	β_c
Roof Collapse	PGA†	0.15–0.17	0.23–0.68	0.85–1.84	0.36–0.61
Diaphragm Failure	PGA	0.10–0.20	0.26–1.13	0.61–2.34	0.30–0.42
Shear Wall with Flexural Failure	PGA	0.10–0.40	0.40–2.28	1.70–4.90	0.28–0.62
Shear Wall with Shear Failure	PGA	0.10–0.40	0.13–1.24	0.44–5.80	0.26–0.72

*Campbell, R.D., M.K. Ravindra, and R.C. Murray. "Compilation of Fragility Information from Available Probabilistic Risk Assessments" UCID–20571. Rev.1. Los Alamos, New Mexico: Lawrence Livermore National Laboratory. 1988.
†Design earthquake, peak ground acceleration

Table 3-4. Fragility data for western U.S. nuclear power plants: Diablo Canyon power plant*

Structure	Plant	$C_{1\%}$† (g)	$C_{50\%}$† (g)	β_r	β_u	β_c‡
Concrete Internal Structure (Internal Structure Shear)	Diablo Canyon	2.98	6.91	0.2	0.31	0.37
Intake Structure (North Wall Shear)	Diablo Canyon	3.23	8.55	0.28	0.31	0.42
Auxiliary Building (North South Shear Wall)	Diablo Canyon	2.67	5.79	0.21	0.26	0.33
Turbine Building (Shear Wall Column 31)	Diablo Canyon	1.84	4.87	0.26	0.33	0.42
Range	Minimum	1.84	4.87	—	—	0.33
	Maximum	3.23	8.55	—	—	0.42

*Pacific Gas and Electric Company. "Final Report of the Diablo Canyon Long Term Seismic Program." Docket Nos. 50-275 and 50-323, Table 6.23. San Francisco, California: Pacific Gas and Electric Company. 1988.
†$C_{1\%}$ (capacity at one percent probability of failure) and $C_{50\%}$ (median capacity) are expressed in terms of 5 percent damped spectral acceleration.
‡Calculated

Table 3-5. Median factor of safety and variability for shear wall components*					
Variable		**Median Safety**	β_r	β_u	β_c†
Capacity Factors					
Ultimate strength versus code allowable	F_S	1.2–2.5	0.06–0.12	0.12–0.18	
Inelastic energy absorption capability	F_μ	1.8–4.0	0.08–0.14	0.18–0.26	
Total capacity factor	$F_C = F_S F_\mu$	2.4–6.0	0.10–0.18	0.22–0.32	
Response Factors					
Modal response					
Design response spectra	F_{SA}	1.2–1.4	0.16–0.22	0.08–0.11	
Damping effects	F_δ	1.2–1.4	0.05–0.10	0.05–0.10	
Modeling effects	F_M	1.0	0	0.12–0.18	
Total modal response factor	$F_{MR} = F_{SA} F_\delta F_M$	1.0	0.10–0.20	0	
Modal and component combination	F_{MC}				
Soil–structure interaction	F_{SSI}	1.1–1.5	0.02–0.06	0.1–0.24	
Total response factor	$F_{RS} = F_{MR} F_{MC} F_{SSI}$	1.6–2.8	0.22–0.32	0.18-0.33	
Factor of Safety‡	$F_m = F_C F_{RS}$	4.0–12.0	0.22–0.37	0.28–0.46	0.36–0.59

*Kennedy, R.P. and M.K. Ravindra. "Seismic Fragilities for Nuclear Power Plant Risk Studies." *Nuclear Engineering and Design*. Vol. 79. pp 47–68. 1984.

†calculated

‡$C_{50\%} = F \cdot DE$, where DE is design earthquake.

4 SENSITIVITY STUDIES

In this section, studies are conducted to understand the sensitivity of parameters on the probability of unacceptable performance of SSCs ITS for regulatory assessment of seismically induced event sequences. Structural elements and equipment were used as SSC ITS components in the analysis.

4.1 Sensitivity on Design Parameter

The probability of unacceptable performance for structural systems located in the Western United States (WUS) and Central and Eastern U.S. (CEUS) designed to applicable codes and standards is evaluated and compared. It is assumed that the design basis ground motion for the WUS structure is 0.42g PGA (where g is acceleration of gravity) and for the CEUS structure it is 0.15g PGA. The fragility parameter's median capacity $C_{50\%}$ and composite logarithmic deviation β_C are evaluated by the Separation of Variable Method using Eq. 3-6. The median factor of safety, $F_{m,}$ for this example is assumed to be 10.0 from the range shown in Table 3-5, and based on the data collected by (Kennedy and Ravindra, 1984). The β_C is assumed to be 0.38 from the range given in Table 3-5. The mean hazard curves representative of the WUS and CEUS are shown in Figure 4-1(a). The mean hazard curve is defined as a function of PGA. The slope of the hazard curves are defined by parameters A_R and $K_{H,}$ as discussed in Section 2.1.1. A_R at any point on the hazard curve is ratio of the ground motion corresponding to a ten-fold reduction in hazard exceedance frequency. Here, hazard exceedance levels at MAPE 1.0 × 10^{-5} and 1.0 × 10^{-6} were used to calculate A_R and $K_H(= 1/\log A_R)$. For the WUS, the A_R and K_H were estimated as 1.57 and 5.13, respectively and for the CEUS 2.04 and 3.22, respectively. These values indicate that hazard curves in the western U.S. are steeper than the CEUS. These curves are shown in Figure 4-1(b), where the hazards curves are normalized at MAPE 1.0 × 10^{-4}. For the CEUS sites, A_R values typically range from 2.0 to 4.5 over the 1.0 × 10^{-4} to 1.0 × 10^{-6} range and for the WUS, the A_R values range from 1.5 to 2.25 over the same frequency of exceedance range (EPRI, 2013). The annual probability of unacceptable performance, P_F, of the structures was estimated by closed form solution for convolving fragility and seismic hazard curves, given in Eq. 2-5. Table 4-1 shows that the P_F of the WUS and CEUS structures are approximately the same order of magnitude at their respective locations. The results also show that the WUS structures have a very low probability of failure (about two orders of magnitude lower) if constructed in the CEUS. Similarly, the CEUS structures have a high probability of failure (about two orders of magnitude higher), if constructed in the WUS.

4.2 Sensitivity on Parameters Affecting P_F

Effects of the critical parameters on the probability of unacceptable performance studied by Dasgupta, et al. (2007) are discussed here. The parameters studied were: (i) closed form solution and numerical integration; (ii) discretization steps in the numerical integration method; (iii) low probability range of the seismic hazard curve; and (iv) log standard deviation of the fragility curve.

Fragility information for HVAC systems was used as generic data for a representative SSC in this analysis. Fragility information was obtained from the published survey of data from probabilistic risk analysis studies for nuclear power plants (Park et al. 1998). Typical failure modes were failure of fan, support, anchor bolts, and base plate. The median fragility range is given as 2.24g–6.9g spectral acceleration. The database does not include information on the

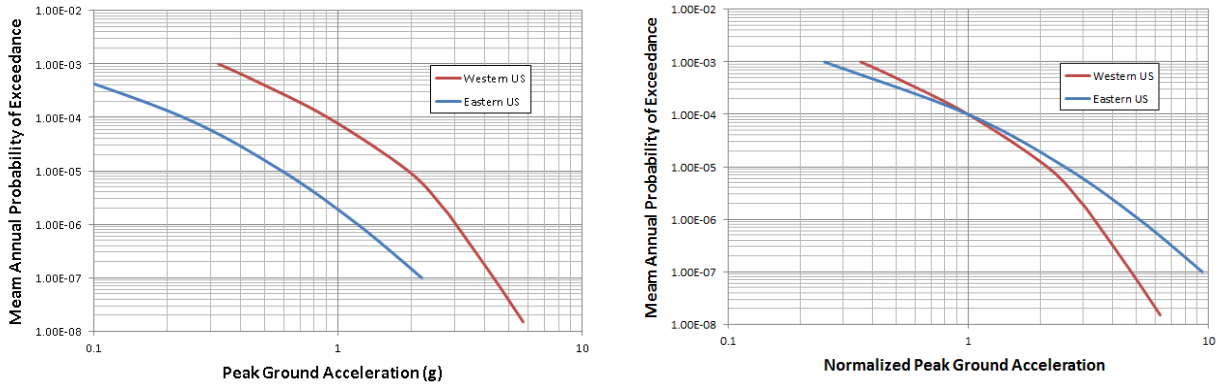

(a) (b)

Figure 4-1. (a) Hazard curves data from the WUS and CEUS and (b) hazard curve data normalized with ground motion at 1 × 10^{-4}

Table 4-1. P_F of structures calculated for the WUS and CEUS

D_{PGA} (g)	F_m	$C_{50\%}$ $(= F_m \cdot D_{PGA})$ (g)	β_C	P_F	
				Western US $A_R = 1.57, K_H = 5.13$	Eastern US $A_R = 2.04, K_H = 3.22$
0.42	10	4.5	0.38	1.27 × 10^{-6}	3.78 × 10^{-8}
0.15	10	1.5	0.38	2.49 × 10^{-4}	1.05 × 10^{-6}

D_{PGA} = Design ground motion, Peak ground acceleration
F_m = Median factor of safety
$C_{50\%}$ = Median Capacity
β_C = Composite or mean logarithmic standard deviation
A_R, K_H = Slope parameters seismic hazard curve
P_F = Annual probability of unacceptable performance
WUS = Western United States
CEUS = Central and Eastern United States

structural frequencies and damping associated with spectral accelerations. The range for random variability, β_R, is 0.20–0.40, and epistemic uncertainty, β_U, is 0.24–0.62 (Park et al. 1998). The range for composite log standard deviation, β_C, was computed to be 0.31–0.74 based on the extreme ranges of β_R and β_U. The median fragility or the capacity of the SSC ITS was assumed to be 3.0g spectral acceleration at 10 Hz structural frequency. A mean fragility curve for $C_{50\%}$ = 3.0g and β_C = 0.4, shown in Figure 4-3, is used as a baseline case for all parametric studies. The estimated $C_{1\%}$ for the baseline fragility curve is 1.183g.

The hazard curve, shown in Figure 4-1, was used in this analysis and is based on the data obtained from the U.S. Geological Survey's (USGS) website for a region in the western U.S. [Dasgupta, et al., 2007]. The hazard data corresponds to a spectral acceleration of 10 Hz. The data from the website were interpolated by statistical line trend techniques to obtain hazard exceedance probability at ten-fold intervals from 1.0 × 10^{-3} to 1.0 × 10^{-7}. Maintaining a constant slope between the 1.0 × 10^{-6} and 1.0 × 10^{-7} probability of exceedance, the hazard curve was extrapolated to 1.0 × 10^{-9}. The hazard curve information obtained from the USGS website is for a firm-rock site condition and does not include seismic ground response considering overlying soil strata at any particular site.

Closed Form Solution and Numerical Integration

In the closed form solution, P_F is estimated by assuming the hazard curve to be linear in the log-log scale. As seen in Eq. 2-5, P_F is controlled by slope parameters K_H and A_R, and constant K_1. The slope parameter A_R at any point on the hazard curve is ratio of the ground motion corresponding to a ten-fold reduction in hazard exceedance frequency. Slope of the hazard curve in Figure 4-2 varies between each ten-fold step of the exceedance probability and Table 4-2 shows the values of A_R, K_H, and K_1 at different hazard levels along the hazard curve. The slope parameter, A_R, varies between 2.17 (shallow) and 1.3 (steep). Using the fragility parameters $C_{50\%}$ = 3.0g and β_C = 0.4 and slope parameters, P_F is estimated by closed form solution. Table 4-2, shows that P_F varies significantly between 3.28×10^{-5} and 4.71×10^{-3}, depending upon which slope on the hazard curve is used. Estimated probability of failure is higher for a steeper slope.

Using numerical integration, P_F is estimated to be 2.26×10^{-5}. The estimated value is closer to the closed form solution for the shallow slope. The difference in the estimated P_F values for the numerical integration and the closed-form expression results from the approximations made on the seismic hazard curve. In the numerical integration, the actual shape of the hazard curve is used within a finite range, whereas in the closed-form solution, the hazard curve is assumed to be a straight line in a log-log scale with a constant slope and integrated over the infinite range (Kennedy and Short, 1994).

Numerical integration can be used to assess the segments of hazard and fragility curves that drive the overall seismic risk. ΔP_F from each discretized segment of the hazard curve is normalized by P_F. The histogram of the normalized ΔP_F and the cumulative distribution is plotted with respect to spectral acceleration, as shown in Figure 4-4. The spectral accelerations in the range of 1.2g to 2.7g contribute approximately 80 percent P_F. This acceleration range corresponds to the MAPE from the hazard curve (Figure 4-2) between 1×10^{-4} and 1×10^{-5}, and the probability of failure (Figure 4-3) between 0.01 to 0.4.

Discretization Steps

The accuracy of P_F , when determined by the numerical integration solution, depends on the number of integration points. The number of integration steps needed to estimate the P_F was examined by Dasgupta, et al. (2007). This study examined the number of integration steps needed to estimate P_F. The discretization step (N) was varied from 6 to 120. The discretization steps cover the entire range of hazard curve 1×10^{-3} and 1×10^{-9} with an equal number of points in each ten-fold interval (e.g., 1.0×10^{-3} to 1.0×10^{-4}) on the hazard exceedance probability. The fragility parameters of $C_{50\%}$ = 3.0g and β = 0.4 were used in this analysis. The results in Table 4-3 show that, for the selected hazard and fragility curves, the numerical integration points of 18 (or 3 points in each tenfold range in the probability of exceedance in the seismic hazard curve) yield reasonable accuracy for estimating P_F. Although a significant number of integration steps are not required in the example presented, sensitivity of integration steps should be examined for accurate estimation of P_F because P_F depends on the shape of both hazard and fragility curves.

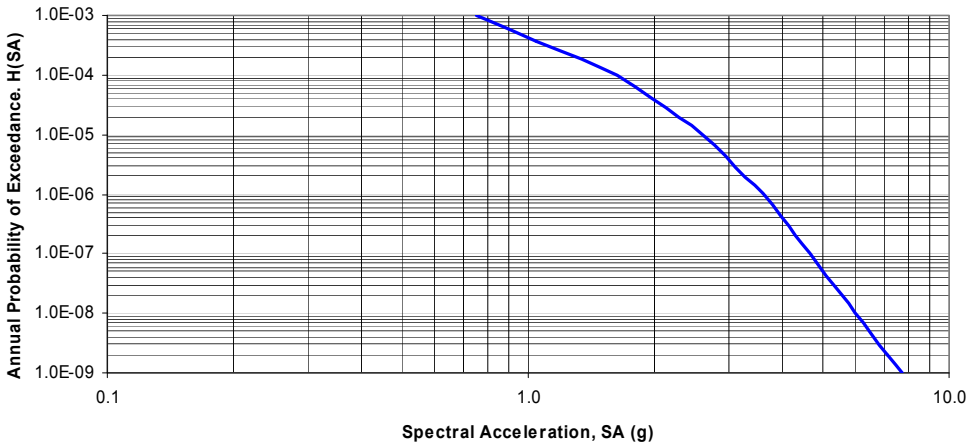

Figure 4-2. Seismic hazard curve—annual probability of exceedance vs spectral acceleration at 10 Hz

Table 4-2. Variation of P_F with hazard curve slope

$H(a)$	Sa	A_R	K_H	K_1	P_F
1.0×10^{-3}	0.753	—	—	—	—
1.0×10^{-4}	1.627	2.17	2.99	4.28×10^{-4}	3.28×10^{-5}
1.0×10^{-5}	2.603	1.6	4.90	1.09×10^{-3}	3.04×10^{-5}
1.0×10^{-6}	3.627	1.4	6.94	7.65×10^{-3}	1.76×10^{-4}
1.0×10^{-7}	4.663	1.3	9.16	1.34×10^{-1}	4.17×10^{-3}

$H(a)$ = MAPE at spectral acceleration *Sa*
Sa= Spectral acceleration
A_R, K_H = Slope parameters and constant and K_1 constant elated to hazard curve
P_F = Mean annual probability of unacceptable performance (or failure) of SSC

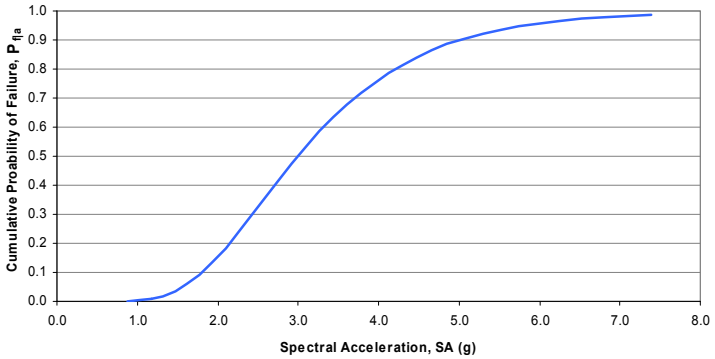

Figure 4-3. Fragility curve with $C_{50\%}$ = 3.0g and β_C = 0.4 for spectral acceleration at 10 Hz

Table 4-3. Effects of discretization steps on P_F		
N	P_F	Ratio = $P_{F,N=n}/P_{F,N=120}$
6	2.081×10^{-5}	0.8835
12	2.235×10^{-5}	0.9785
18	2.263×10^{-5}	0.9908
24	2.272×10^{-5}	0.9947
30	2.277×10^{-5}	0.9969
60	2.283×10^{-5}	0.9996
120	2.284×10^{-5}	1.0000

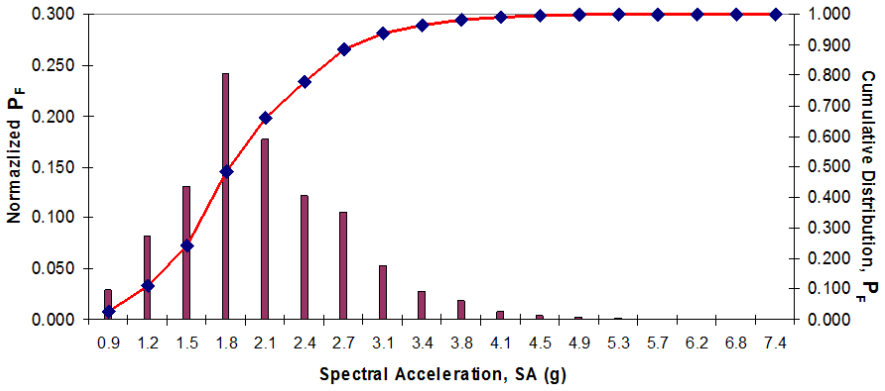

Figure 4-4. Histogram and cumulative distribution of P_F vs spectral acceleration

Low Probability Range of Hazard Curve

In numerical integration, a hazard curve should include a reasonable range of ground motion intensities for estimating probability of unacceptable performance of an SSC. The sensitivity of the seismic risk of SSC ITS to the range of probability of exceedance in the hazard curve was explored by Dasgupta, et al. (2007) using numerical integration. The hazard curve range was terminated at 1×10^{-5}, 1×10^{-6}, 1×10^{-7}, 1×10^{-8}, and 1×10^{-9} probabilities of exceedance. P_F for each case is shown in Table 4-4. The fragility curve, shown in Figure 4-2, is used in this analysis, and the number of integration points is N = 18. The effect of range of hazard curve is indicated by the ratio column, which shows the ratio of P_F at hazard exceedance probability, $H(Sa)$, to the P_F at $H(Sa)$= 1×10^{-9}. The results indicate that hazards at an exceedance level below 1.0×10^{-7} have no significant effect on P_F. In this example, P_F at exceedance level 1×10^{-6} or 1×10^{-7} approaches the values at the lower exceedance level of 1×10^{-9}. However, hazard curves with exceedance level lower than 1×10^{-7} may have significant contribution on P_F when convolved with fragility curves with a long tail. Sensitivity of range of the hazard curve should be examined for accurate estimation of P_F.

Table 4-4. Effect of variation of lower boundary of hazard curve		
Annual Probability of Exceedance of Hazard Curve, $H(Sa)$	**Annual Probability of Unacceptable Performance, P_F**	**Ratio $P_{F,H(Sa)} / P_{F,H(1.0\times10^{-9})}$**
1.0×10^{-5}	1.766×10^{-5}	0.78
1.0×10^{-6}	2.186×10^{-5}	0.97
1.0×10^{-7}	2.254×10^{-5}	0.99
1.0×10^{-8}	2.262×10^{-5}	1.0
1.0×10^{-9}	2.263×10^{-5}	1.0

Log Standard Deviation

The influence of β_C on P_F considering fragility curves based on $C_{50\%}$ and $C_{1\%}$ capacities was studied by Dasgupta et al. (2007). The log standard deviation β_C was varied from 0.3 to 0.6, consistent with the ranges suggested by ASCE (2005). Figure 4-5 shows a plot of several fragility curves with $C_{50\%}$ = 3.0g and for different values of β_C. Convolving the fragility curves with the hazard curves in Figure 4-2 by numerical integration, the variation of P_F with β_C is given in Table 4-5, and shown in Figure 4-7. As expected, the results show the mean probability of unacceptable performance increases with increasing composite uncertainty β_C. The estimated values of P_F for β_C ranging from 0.4 to 0.6 are about 2 to 5 times higher than at β_C = 0.3.

Fragility curves anchored at $C_{1\%}$ = 1.183g and β_C ranging from 0.3 to 0.6 are shown in Figure 4-6. The median capacity $C_{50\%}$ is computed using Eq. 3-3 and P_F is obtained by convolving fragility curves in Figure 4-6 with seismic hazard curves in Figure 4-2 by numerical integration. The estimated P_F is given in Table 4-5 and the variation with β_C is shown in Figure 4-7. As seen in Figure 4-6, when the fragility is anchored at $C_{1\%}$ the median capacity increases with increasing composite uncertainty β_C, shifting the fragility curve to the right and the P_F decreases with increasing $\beta_{C,}$ as seen in Figure 4-7. Contrary to expectation, the probability of failure, P_F, gets better with increasing composite uncertainty because of the property of lognormal distribution. The decrease in P_F, however, ranges between 1.6 (β_C = 0.4) to 2.7 (β_C = 0.6) times with respect to β_C = 0.3. Hence, while estimating fragility by the CDFM approach, overestimating β_C may not be conservative because it increases $C_{50\%}$. If the numerical value of P_F is at or close to the event sequence categorization limit, realistic estimation or defensible basis for β_C is necessary.

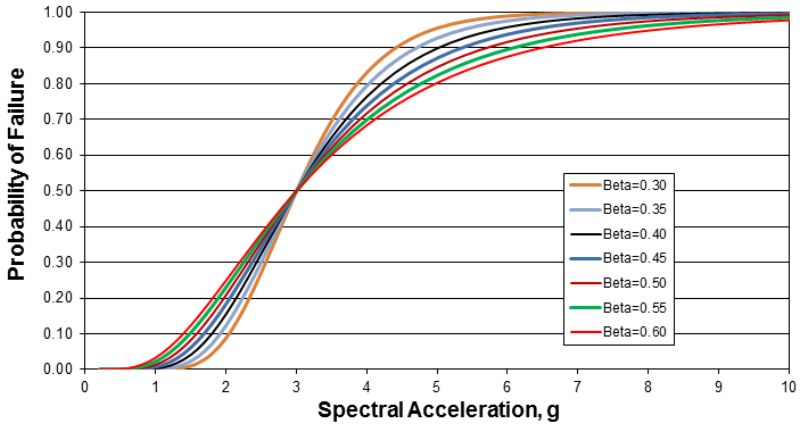

Figure 4-5. Fragility curves anchored at $C_{50\%}$ = 3.0g

Table 4-5. Values of P_F with varying β_C		
	P_F	
β_C	$C_{50\%} = 3.0\ g$	$C_{50\%} = 1.183\ g$
0.3	1.27×10^{-5}	3.56×10^{-5}
0.35	1.70×10^{-5}	2.78×10^{-5}
0.4	2.25×10^{-5}	2.26×10^{-5}
0.45	2.95×10^{-5}	1.89×10^{-5}
0.5	3.08×10^{-5}	1.65×10^{-5}
0.55	4.78×10^{-5}	1.47×10^{-5}
0.6	5.87×10^{-5}	1.34×10^{-5}
P_F = Annual probability of unacceptable performance		

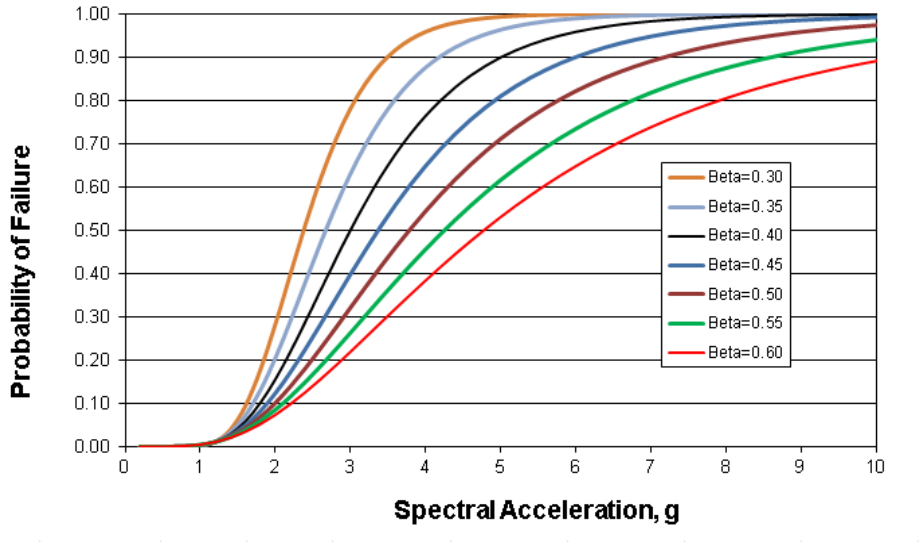

Figure 4-6. Fragility curves anchored at $C_{1\%}$ = 1.183g

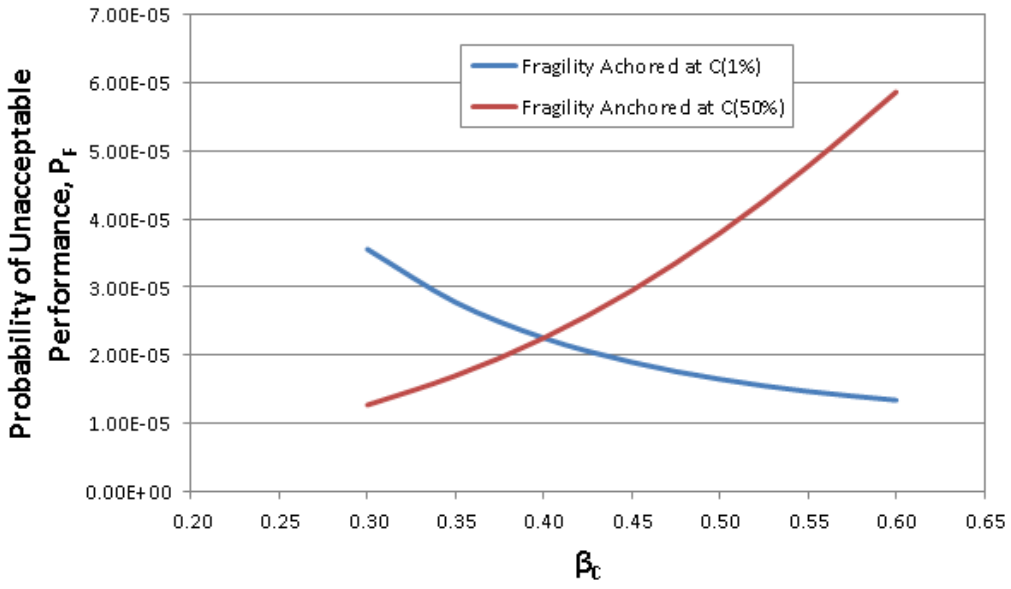

Figure 4-7. Probability of unacceptable performance (P_F) vs composite uncertainty (β_C)

5 SUMMARY

DOE identified seismicity as a credible natural hazard at the Yucca Mountain site. Thus, DOE identified and characterized seismically initiated event sequences that could potentially disrupt safe operations at the GROA during the preclosure period.

The GROA surface facilities design included several building structures with various types of mechanical equipment (e.g., overhead cranes, trolleys, transporters) for loading, unloading, and transferring of casks, canisters, waste packages, and spent fuel assemblies. The mechanical equipment is supported by other systems such as HVACs, electrical cabinets (containing relays), piping systems, roll-up doors, and shield doors. In the proposed repository facility, initiation of disruptive event sequences may be caused by seismically induced failure of equipment (e.g. a crane) impacting a waste container and leading to eventual loss of containment or breach of the waste container, due to mechanical impacts. If, in addition, the concrete building structure and HVAC systems fail, release of radioactive material to the environment may occur.

NRC issued ISG HLWRS-ISG-01 (NRC, 2006) to support the review of seismically initiated event sequences in the preclosure safety analysis. The review methodology considers the likelihood of seismic initiating events at the site and the fragility of SSCs ITS, to estimate probability of failure of SSCs ITS and frequency of occurrence of event sequences. Seismic fragility of a structure or equipment is defined as the conditional probability of failure for a given level of seismic ground motion. These ground motions may be defined as either the peak ground acceleration (PGA) or a spectral acceleration (Sa). The probability of occurrence of an event sequence caused by failure or unacceptable performance of the individual SSC ITS is estimated by convolving (or integrating) the mean seismic hazard curve with the mean fragility curve. If the probability of failure values of individual SSCs ITS for seismically initiated event sequences is less than 1 in 10,000 during the preclosure period, for Category 2 event sequences, the SSC ITS is considered to perform its intended safety function, thereby meeting the performance objectives in 10 CFR Part 63. If, however, the probability of failure of the individual SSCs ITS for seismically initiated event sequences is greater than or equal to 1 in 10,000 during the preclosure period, event progression can be analyzed by assessing subsequent success or failure of individual SSCs relied on to prevent or mitigate the event sequences. The fragilities of SSCs in an event sequence can be combined using Boolean logic. The resulting combined fragility for the sequence is convolved with hazard curves to compute the event sequence frequency. Compliance with 10 CFR 63 can be demonstrated by showing that the probability of occurrence of each seismic event sequences is less than 1 in 10,000 during the preclosure period. If the event sequence frequency is greater than 1 in 10,000, regulatory compliance can still be met by showing that the dose consequence to the public at the site boundary arising from the specific event sequence is less than the dose limits in 10 CFR 63.111(b)(2). However, DOE's approach to demonstrate preclosure safety in its Yucca Mountain Safety Analysis Report is solely based on quantification of event sequences and showing that the event sequence frequency is less than the Category 2 (thus, full dose consequence evaluations were not required).

Seismic fragility of a structure or equipment is defined as the conditional probability of failure for a given level of seismic ground motion (defined as the PGA or Sa). The fragility curve is typically described by a lognormal distribution that is defined by the median capacity, $C_{50\%}$, and the natural logarithmic standard deviation, which may be separated into epistemic uncertainty, β_U, and random variability, β_R. The mean fragility curve is a single curve defined by median capacity, $C_{50\%}$, and composite logarithmic standard deviation β_C. The fragility evaluation

includes estimation of seismic demand on the structures from response analyses, and the capacity of the structural systems and equipment to withstand the demand. Seismic response involves dynamic modeling of ITS surface facility structures to define seismic demands (e.g., bending moment, shear force) on structural components, as well as floor acceleration. Floor acceleration is used to develop in-structure response of individual equipment, and compute demand forces. Fragility curves of components are then developed for a given failure mode. If a structure can fail in multiple failure modes (e.g., failure modes for concrete shear wall are diagonal shear cracking, flexure, and shear friction), all failure modes must be investigated and the fragility of the structure is estimated based on the lowest capacity of the possible failure modes. Equipment and component failure modes include anchorage, functional failures, and failure due to seismic interactions.

Two approaches are commonly used in developing mean fragility curves: (i) CDFM Method and (ii) separation of variables method. If HCLPF is independently estimated and β_C is selected based on judgement, the mean fragility is a cumulative lognormal distribution with HCLPF as the 0.01 quantile and β_C as its logarithmic standard deviation. The parameter $C_{50\%}$ is the median of such distribution. The HCLPF, is estimated using the CDFM method. In the separation of variables method, the median capacity, $C_{50\%,}$, including epistemic uncertainty, β_U, and random variability, β_R, are estimated for structures and equipment. The mean fragility curve is developed using $C_{50\%,}$, and the composite logarithmic standard deviation, β_C. The fragility parameters are calculated considering the contributions of various capacity and demand or response parameters.

The application of these fragility methods to determine the likelihood of adverse events and event sequences requires a careful characterization of the associated uncertainties, and potential inaccuracies arising from mathematical simplifications of the analyses. The sensitivity of various parameters affecting the probability of unacceptable performance of SSCs (P_F) and seismic risk were explored in this report. It is concluded that P_F values computed with closed form equations tend to be higher than when computed by numerical integration, especially when the seismic hazard curve is relatively steep. The difference arises predominantly from approximations to simplify the seismic hazard curve. In the numerical integration, the actual shape of the hazard curve is used within a finite range of exceedance frequencies, whereas in the closed-form solution, the hazard curve is assumed to be a straight line in a log-log scale, and integrated over the full range of exceedance frequencies from zero to infinity. Based on the sensitivity study, a limited number of integration steps can provide reasonable accuracy in the numerical integration. Assessment of low probability range of the hazard curve on P_F shows that the contribution from a seismic hazard curve below annual probability of exceedance 10^{-7} was negligible, at least for the range of fragility values analyzes considered in this report. When the fragility curve is based on $C_{50\%}$, P_F increases with increasing values of the β_C parameter, as expected. However, when the fragility curve of SSC ITS is based on $C_{1\%}$, P_F decreases with increasing β_C because of the property of lognormal distribution. Although P_F may not be highly sensitive to β_C , when the numerical value of P_F is close to the category limit or performance objective, a realistic estimation and defensible basis for β_C is critical to a robust evaluation of risk.

6 REFERENCES

ASCE. "Seismic Design Criteria for Structures, Systems, and Components in Nuclear Facilities." ASCE/SEI 43-05. Reston, Virginia: American Society of Civil Engineers, Structural Engineering Institute. 2005.

ASCE. "Seismic Analysis of Safety-Related Nuclear Structures." ASCE 4-98. Reston, Virginia: American Society of Civil Engineers, Structural Engineering Institute. 1998.

Campbell, R.D., M.K. Ravindra, and R.C. Murray. "Compilation of Fragility Information from Available Probabilistic Risk Assessments." UCID-20571, Rev.1. Los Alamos, New Mexico: Lawrence Livermore National Laboratory. 1988.

Dasgupta, B., M.J. Shah, and A.H. Chowdhury. "Sensitivity of Parameters Affecting Seismic Rock." 19th International Conference on Structural Mechanics in Reactor Technology (SMiRT–19). Toronto, Canada: International Association for Structural Mechanics in Reactor Technology. August 12–17, 2007.

DOE. "Preclosure Seismic Design and Performance Demonstration Methodology for a Geologic Repository at Yucca Mountain Topical Report." YMP/TR–003–NP, Revision 5. ML072060663. Las Vegas, Nevada: U.S. Department of Energy, Office of Civilian Radioactive Waste Management. 2007.

EPRI. "Seismic Evaluation Guidance – Screening Priorities and Implementation Details (SPID) for Resolution of Fukushima Near-Term Task Force Recommendation 2.1: Seismic." Palo Alto, California: Electric Power Research Institute. 2013.

———. "Seismic Fragility Applications Guide Update." Final Report EPRI 1019200. Palo Alto, California: Electric Power Research Institute. 2009.

———. "Methodology for Developing Seismic Fragilities." Report EPRI TR–103959. Palo Alto, California: Electric Power Research Institute. 1994.

———. "A Methodology for Assessment of Nuclear Power Plant Seismic Margin." Final Report EPRI NP–6041–SL. Rev 1. Project 2722–23. Palo Alto, California: Electric Power Research Institute. 1991.

Kennedy, R.P. "Risk Based Seismic Design Criteria." *Nuclear Engineering and Design*. Vol. 192. pp. 117–135. 1999a.

———. "Overview of Methods for Seismic PRA and Margin Analysis Including Recent Innovations." OECD/NEA Workshop on Seismic Risk, Tokyo, Japan, August 10–12, 1999b.

Kennedy, R.P. and S.A. Short. "Basis for Seismic Provisions of DOE STD–1020." UCRL–CR–111478. Washington, DC: DOE. 1994.

Kennedy, R.P. and M.K. Ravindra. "Seismic Fragilities for Nuclear Power Plant Risk Studies." *Nuclear Engineering and Design*. Vol. 79. pp. 47–68. 1984.

Kennedy, R.P., C.A. Cornell, R.D. Campbell, S. Kaplan, and H.F. Perla. "Probabilistic Seismic Study of an Existing Nuclear Power Plant." *Nuclear Engineering and Design*. Vol. 59. pp. 315–338. 1980.

McGuire, R. "Seismic Hazard and Risk Analysis." Oakland, California: Earthquake Engineering Research Institute. 2004.

NRC. NUREG–0800, "Standard Review Plan for the Review of Safety Analyses Reports for Nuclear Power Plants." Revision 3. Washington, DC: NRC. March 2007a.

_____. "Preclosure Safety Analysis—Level of Information and Reliability Estimation." Division of High-Level Waste Repository Safety, Interim Staff Guidance HLWRS–ISG–02. Washington, DC: NRC. 2007b.

_____. "Review Methodology for Seismically Initiated Event Sequences." Division of High-Level Waste Repository Safety, Interim Staff Guidance HLWRS–ISG–01. Washington, DC: NRC. 2006.

_____. NUREG–1742, "Perspective Gained from Individual Plant Examination of External Events (IPEEE) Program." Volumes. 1 and 2. Washington, DC: NRC. November 2002.

_____. NUREG–1407, "Procedure and Submittal Guidance for Individual Plant Examination of External Events (IPEEE) for Severe Accident Vulnerabilities." Washington, DC: NRC. June, 1991.

Pacific Gas and Electric Company. "Final Report of the Diablo Canyon Long Term Seismic Program." Docket Nos. 50-275 and 50-323, Table 6.23. San Francisco, California: Pacific Gas and Electric Company. 1988.

Park, Y. J., C.H. Hofmayer, and N.C. Chokshi. "Survey of Seismic Fragilities Used in PRA Studies of Nuclear Power Plants." *Reliability and Systems Safety*. Vol. 62. pp. 183–195. 1998.